Electronic Communication in Homobimetallic Anthracene-Bridged η^5-Cyclopentadienyl Derivatives of Rhodium(I): Generation and Characterization of the Average-Valence Species $[L_2Rh\{C_5H_4CH_2(9,10\text{-anthrylene})CH_2C_5H_4\}RhL_2]^+$

Maurizio Carano,[†] Maria Careri,[‡] Francesca Cicogna,[§] Irene D'Ambra,[§] Julien L. Houben,[∥] Giovanni Ingrosso,[§,*] Massimo Marcaccio,[†] Francesco Paolucci,[†] Calogero Pinzino,[∥] and Sergio Roffia[†]

Dipartimento di Chimica "G. Ciamician", Università di Bologna, Via Selmi 2, 40126 Bologna, Italy, Dipartimento di Chimica Generale ed Inorganica, Chimica Analitica, Chimica Fisica, Parco Area delle Scienze 17/A, 43100 Parma, Italy, Dipartimento di Chimica e Chimica Industriale, Università di Pisa, Via Risorgimento 35, 56126 Pisa, Italy, and Istituto di Chimica Quantistica ed Energetica Molecolare del CNR, Area della Ricerca di Pisa, Via G. Moruzzi 1, 56010 Ghezzano San Giuliano Terme (Pisa), Italy

Received March 15, 2001

9,10-Bis(cyclopentadienylmethyl)anthracene (**1**) is obtained by reacting 9,10-bis(bromomethyl)anthracene with cyclopentadienylsodium and transformed into its dithallium(I) derivative **3** on reaction with thallium ethoxide. The reaction of **3** with the chloro derivatives of rhodium(I) of formula $[RhClL_2]_2$ (L = η^2-C_2H_4 or CO; L_2 = η^4-C_7H_8) leads to the corresponding bimetallic complexes $[L_2Rh\{C_5H_4CH_2(9,10\text{-anthrylene})CH_2C_5H_4\}RhL_2]$, **4** (L = η^2-C_2H_4), **5** (L = CO), and **6** (L_2 = η^4-C_7H_8), in 13, 22, and 55% yields, respectively. All complexes have been characterized by elemental analysis, particle beam mass spectrometry, ^{1}H NMR, and FT-IR. The UV−vis spectra (280−800 nm) of **4**−**6** are indicative of the existence of strong electronic interactions among the anthrylic chromophore and the two cyclopentadienylRhL_2 moieties. When excited at ca. 370 nm, **1** becomes an efficient light-emitting molecule, while **4**−**6** are poorly luminescent compounds. The fluorescence spectra of all the complexes present the vibrational structure typical of the anthrylic fluorophore but have low intensity: 6, 3, and 15% of the one observed for 9-methylanthracene, taken as the reference compound, respectively for **4**, **5**, and **6**. The study of the electrochemical behavior of **4**−**6** in strictly aprotic conditions allows a satisfactory interpretation of the observed electrode processes and furnishes information about the location of the redox sites along with the thermodynamic characterization of the corresponding redox processes. These data show that the occurrence of an intramolecular charge-transfer process between the photoexcited 9,10-anthrylenic moiety and the cyclopentadienylRhL_2 unit is a possible route for the observed quenching of emission in the compounds **4**−**6**. The one-electron oxidation of compounds **4**−**6** by thallium(III) trifluoroacetate in a 1:1 dichloromethane/1,1,1,3,3,3-hexafluoropropan-2-ol mixture leads to the formation of the corresponding radical cations $[L_2Rh\{C_5H_4CH_2(9,10\text{-anthrylene})CH_2C_5H_4\}RhL_2]^+$. Two of them, i.e., $\mathbf{4}^+$ (L = η^2-C_2H_4) and $\mathbf{5}^+$ (L = CO), give rise to highly resolved EPR spectra which allow one to describe such species as average-valence [$Rh^{+1/2}$, $Rh^{+1/2}$] complexes. DFT calculations of spin density distribution confirm the EPR results and allow a further insight into the structure of $\mathbf{4}^+$ and $\mathbf{5}^+$ complexes.

1. Introduction

The presence of two or more active sites within the same molecular skeleton allows for the so-called cooperative effect to occur. This may result either in a significant modification of individual properties or in the appearance of novel properties that are not observed for monofunctional compounds. In fact, a strong electronic communication between linked active sites may magnify a series of phenomena.[1] Consequently, a great interest has been aroused for systems of this type with the aim to synthesize new molecular species with novel chemical and physical properties that allow for the preparation of new products, new and more efficient catalytic systems, and new materials for use in electronics and

* To whom correspondence should be addressed. E-mail: vanni@dcci.unipi.it.
[†] Università di Bologna.
[‡] Parco Area delle Scienze 17/A.
[§] Università di Pisa.
[∥] Istituto di Chimica Quantistica ed Energetica Molecolare del CNR.

(1) Balzani, V.; Campagna, S.; Denti, G.; Juris, A.; Serroni, S.; Venturi, M. *Acc. Chem. Res.* **1998**, *31*, 26.

10.1021/om010206o CCC: $20.00
Publication on Web 07/03/2001

telecommunications (molecular conductors, nonlinear optics, molecular devices, photoswitches, etc.).[1,2] In transition metal derivatives the cooperative effect often manifests as a marked increase of the reactivity of the metal centers.[3] In this connection, an important role is played by the spacer, or bridging ligand, that links the sites, which must be able to maximize the transmission of electronic effects from one site to another.[4] In monometallic complexes in which the metal-containing moiety is linked to an organic functional group, behaving as an *antenna*, the chemical behavior as well as the physical properties (luminescence, fluorescence, nonlinear optical activity, charge transfer, redox properties, etc.) of the antenna often change quite notably.[5] In polymetallic complexes, in which it is possible to analyze the effects of chemical, electrochemical, or photochemical modifications of a metal center on the properties of the other, the reciprocal interaction between the active centers often brings surprising results. Among the phenomena that have been increasingly studied are the chemical and electrochemical transport of electrons and energy.[2c] Recent research has been focused on the class of bis(η^5-cyclopentadienyl)M complexes such as ferrocenyl.[6] It is possible to foresee numerous potential applications for these systems, which are characterized by intermetallic interactions. Important efforts in this direction can be found in the work of Katz and coworkers,[7] who have studied various metallocenyl polymers based on "helicene" ligands as potential "chiral conductors of electricity". Another class of complexes that has been investigated is that in which two cyclopentadienyl−metal moieties are linked by a σ-bond (fulvalene series) or by a hydrocarbon chain.[8]

We have recently synthesized several new molecular species in which a cyclopentadienyl−metal moiety is connected to a fluorophoric fragment behaving as an antenna, having the following structure:[9]

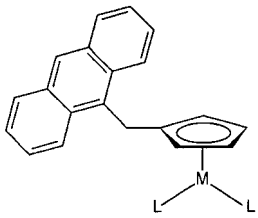

M = Rh, Ir;
L = olefins, CO, PPh_3

Compounds of this type allowed us to test how the active sites communicate in those conditions (chemical, photochemical, or electrochemical) that can induce the intramolecular transmission of electronic effects. We found that the cyclopentadienyl−metal system can behave as a control unit capable of modifying the physical properties characteristic of the athracenic fluorophore. We have now extended this study to bimetallic systems and have synthesized new complexes in which the 9,10-anthrylene moiety is linked to two cyclopentadienyl−metal moieties:

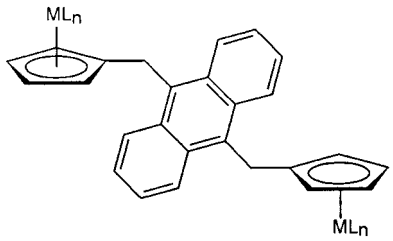

We have started a study to test how the presence of two cyclopentadienyl−metal components influences the physical properties of the fluorophore and if and how the two metal centers can communicate electronically.

This paper deals with some homo-bimetallic derivatives of rhodium(I). Within the great area concerning the synthesis and the study of luminescent and redox-active polynuclear transition metal complexes a very few papers deal with rhodium derivatives.[2a,10]

2. Results and Discussion

2.1. Preparation of Bimetallic Anthracene-Bridged Cyclopentadienyl Derivatives of Rho-

(2) (a) Balzani, V.; Scandola, F. *Supramolecular Photochemistry*; Ellis Horwood: New York, 1991. (b) Bissel, R. A.; De Silva, A. P.; Gunaratne, H. Q. N.; Lynch, P. L.; Maguire, G. E.; McCoy, C. P.; Sandanayake, K. R. A. S. *Top. Curr. Chem.* **1993**, *168*, 223. (c) Ward, M. D. *Chem. Soc. Rev.* **1995**, *24*, 121. (d) Lehn, J. M. *Supramolecular Chemistry. Concepts and Perspectives*; VCH: Weinheim, 1995. (e) Fabbrizzi, L.; Liccarelli, M.; Pallavicini, P.; Perotti, A.; Taglietti, A.; Sacchi, D. *Chem. Eur. J.* **1996**, *2*, 75. (f) De Silva, A. P.; Gunaratne, H. Q. N.; Gunnlaugsson, T.; Huxley, A. J. M.; McCoy, C. P.; Rademacher, J. T.; Rice, T. E. *Chem. Rev.* **1997**, *97*, 1515. (g) De Cola, L.; Belser, P. *Coord. Chem. Rev.* **1998**, *177*, 301. (h) Bergonzi, R.; Fabbrizzi, L.; Licchelli, M.; Mangano, C. *Coord. Chem. Rev.* **1998**, *170*, 31. (i) Daffy, L. M.; De Silva, A. P.; Gunaratne, H. Q. N.; Huber, C.; Lynch, P. L. M.; Werner, T.; Wolfbeis, O. S. *Chem. Eur. J.* **1998**, *4*, 1810. (j) Prodi, L.; Bolletta, F.; Montalti, M.; Zaccheroni, N. *Eur. J. Inorg. Chem.* **1999**, 455. (k) Collins, G. E.; Choi, L.-S.; Ewing, K. J.; Michelet, V.; Bowen, C. M.; Winkler, J. D. *J. Chem. Soc., Chem. Commun.* **1999**, 321. (l) Fabbrizzi, L.; Gatti, F.; Pallavicini, P.; Zambarbieri, E. *Eur. Chem. J.* **1999**, *5*, 682. (m) Knoblauch, S.; Hartl, F.; Stufkens, D. J.; Hennig, H. *Eur. J. Inorg. Chem.* **1999**, 303. (n) Fabbrizzi, L.; Licchelli, M.; Parodi, L.; Poggi, A.; Taglietti, A. *Eur. J. Inorg. Chem.* **1999**, 35. (o) Nakashima, K.; Miyamoto, T.; Hashimoto, S. *J. Chem. Soc., Chem. Commun.* **1999**, 213. (p) Pina, F.; Maestri, M.; Balzani, V. *J. Chem. Soc., Chem. Commun.* **1999**, 107. (q) Barlow, S.; Marder, S. R. *Chem. Commmun.* **2000**, 1555. (r) Rouzaud, J.; Castel, A.; Rivière, P.; Gornitzka, H.; Manriquez, J. M. *Organolmetallics* **2000**, *19*, 4678.

(3) (a) Bonifaci, C.; Carta, G.; Ceccon, A.; Gambaro, A.; Santi, S.; Venzo, A. *Organometallics* **1996**, *15*, 1630. (b) Mantovani, L.; Ceccon, A.; Gambaro, A.; Santi, S.; Ganis, P.; Venzo, A. *Organometallics* **1997**, *16*, 2682. (c) Lo Sterzo, C. *Synlett.* **1999**, 1704.

(4) Balzani, V.; Juris, A.; Venturi, M.; Campagna, S.; Serroni, S. *Chem. Rev.* **1996**, *96*, 759.

(5) Davis, R.; Kane-Maguire, L. A. P. *Comprehensive Organometallic Chemistry*; Wilkinson, G., Stone, F. G. A., Eds.; Pergamon Press Ltd.: New York, 1982; Chapter 26.2, pp 1045−1051.

(6) (a) Long, N. J. *Metallocenes. An Introduction to Sandwhich Complexes*; Blackwell Science: Oxford, 1998. (b) Astruc, D. *Acc. Chem. Res.* **1997**, *30*, 383.

(7) (a) Katz, T. J.; Sudhakar, A.; Tessley, M. F.; Gilbert, A. M.; Geiger, W. E.; Robben, M. P.; Wuensch, M.; Ward., M. D. *J. Am. Chem. Soc.* **1993**, *115*, 3182. (b) Gilbert, A. M.; Katz, T. J.; Geiger, W. E.; Robben, M. P.; Rheingold, A. L. *J. Am. Chem. Soc.* **1993**, *115*, 3199.

(8) (a) Diederich F.; Rubin, Y. *Angew. Chem., Int. Ed. Engl.* **1992**, *31*, 1101. (b) Beck, W.; Niemer B.; Wiser, M. *Angew. Chem., Int. Ed. Engl.* **1993**, *32*, 923. (c) Lang, H. *Angew. Chem., Int. Ed. Engl.* **1994**, *34*, 547. (d) Bunz, U. *Angew. Chem., Int. Ed. Engl.* **1996**, *35*, 969. (e) Kerber, R. C.; Waldbaum, B. R. *J. Organomet. Chem.* **1996**, *513*, 277. (f) Fierro, R.; Bitterwolf, T. E.; Rheingold, A. L.; Yap, G. P. A.; Liable-Sands, L. M. *J. Organomet. Chem.* **1996**, *524*, 19. (g) Kovács I.; Baird, M. C. *Organometallics* **1996**, *15*, 3588. (h) Lee, S. S.; Lee, T.-Y.; Lee, J. E.; Lee, I.-S.; Chung, Y. K. *Organometallics* **1996**, *15*, 3664. (i) Behrens, U.; Brussard, H.; Hagenau, U.; Heck, J.; Hendrickx, E.; Körnich, J.; van der Linden, J. G. M.; Parsoons, A.; Spek, A. L.; Veldman, N.; Vos, B.; Wong, H. *Chem. Eur. J.* **1996**, *2*, 98. (j) Brady, M.; Weng, W.; Zhou, Y.; Seyler, J. W.; Amoroso, A. J.; Arif, A. M.; Böhme, M.; Frenking, G.; Gladysz, J. A. *J. Am. Chem. Soc.* **1997**, *119*, 775. (k) Belanzoni, P.; Re, N.; Sgamellotti, A.; Floriani, C. *J. Chem. Soc., Dalton Trans.* **1998**, 1825.

(9) Cicogna, F.; Colonna, M.; Houben, J. L.; Ingrosso, G.; Marchetti, F. *J. Organomet. Chem.* **2000**, *593*−*594*, 251.

(10) Barigelletti, F.; Flamigni, L. *Chem. Soc. Rev.* **2000**, *29*, 1.

Table 1. ^{1}H NMR Data for 9,10-Bis(cyclopentadienylmethyl)anthracene, 1[a]

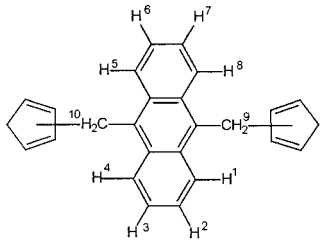

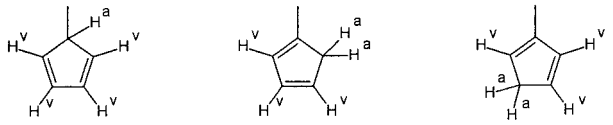

protons	δ (ppm), J/Hz
H^1, H^4, H^5, H^8	8.37−8.16, 4 H, m
H^2, H^3, H^6, H^7	7.40−7.22, 4 H, m
H^9, H^{10}	4.68−4.48, 4 H, broad split signal
H^v	6.62−6.53, m; 6.33−6.23, m; 6.16−6.08, m; 5.97, bs; 5.67−5.61, m
H^a	2.80−2.72, m; 2.72−2.56, m

[a] Spectra recorded in C_6D_6; m = multiplet; bs = broad signal.

dium(I) 4−6. The synthesis of 9,10-bis(cyclopentadienylmethyl)anthracene (**1**), a simple bifunctionalized anthracene derivative, was performed by reacting 9,10-bis(bromomethyl)anthracene (**2**)[11] with cyclopentadienylsodium (eq 1). Column chromatography of the crude reaction product afforded **1** as a spectroscopically pure yellow solid, which was characterized by elemental analysis, ^{1}H NMR, and EI mass spectrometry.

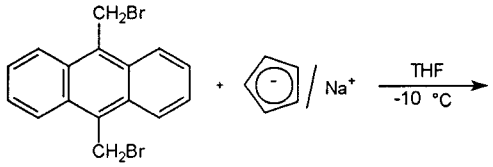

2

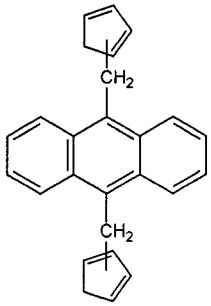

1 (1)

Six isomeric structures are possible for **1**. Accordingly, its ^{1}H NMR spectrum is quite complex. Indeed, apart from the aromatic protons, which give rise to the expected pattern for a 9,10-anthrylene moiety, the vinylic and allylic protons of the cyclopentadiene rings, owing to the presence of isomers, give rise to two sets of broad signals (Table 1). The resonances due to the vinylic protons range from δ 6.62 to 5.61 ppm, and those arising from the allylic protons are observed in the range δ 2.80−2.56 ppm. Finally, the broad split signal, ranging from δ 4.68 to 4.48 ppm, is attributed to the two methylene groups that connect the anthrylic moiety with the C_5 rings.

By reacting **1** with thallium ethoxide in absolute ethanol, at room temperature, 9,10-bis[(cyclopentadienylmethyl)thallium(I)]anthracene (**3**) (eq 2) was obtained as an ochre-yellow solid that can be stored under dinitrogen at room temperature for long periods of time without apparent decomposition.

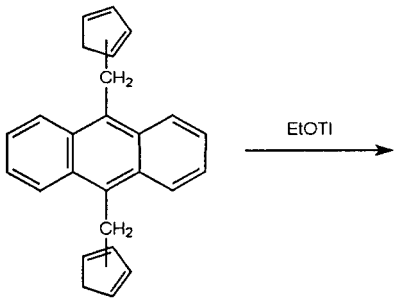

1

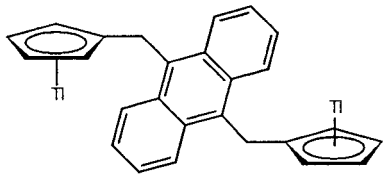

3 (2)

The reaction of **3** with $[RhClL_2]_2$ (L = η^2-C_2H_4 or CO; L_2 = η^4-C_7H_8) produced the bimetallic derivatives **4**−**6** of general formula $[L_2Rh\{C_5H_4CH_2$(9,10-anthrylene)$-CH_2C_5H_4\}RhL_2]$ (L = η^2-C_2H_4, **4**; L = CO, **5**; L_2 = η^4-C_7H_8, **6**) (eq 3).

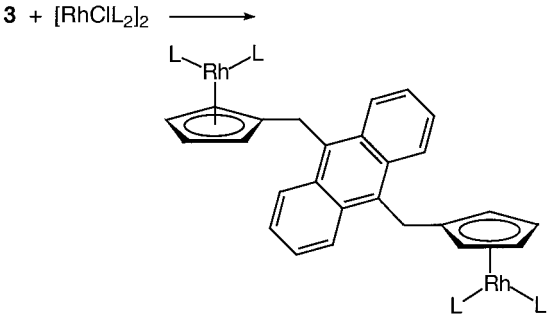

4, L = η^2-C_2H_4
5, L = CO
6, L_2 = η^4-C_7H_8 (3)

Compounds **4**−**6** are sufficiently thermally stable in the solid state to be manipulated at room temperature under dinitrogen without apparent decomposition. Anyway, **6** is markedly more stable than **5**, which in turn is more stable than **4**. Notably, the yields obtained in the three cases (55, 22, and 13%, respectively) decrease in the same order. The new complexes were characterized by elemental analysis, ^{1}H NMR, mass spectrometry, and, where appropriate, also FT-IR. In all cases,

(11) Ashton, P. R.; Ballarini, R.; Balzani, V.; Boyd, S. E.; Credi, A.; Gandolfi, M. T.; Gómez-López, M.; Iqbal, S.; Philp, D.; Preece, J. A.; Prodi, L.; Ricketts, H. G.; Stoddart, J. F.; Tolley, M. S.; Venturi, M.; White, A. J. P.; Williams, D. J. *Chem. Eur. J.* **1997**, *3*, 167.

Table 2. ^{1}H NMR Data for the Complexes 4−6[a]

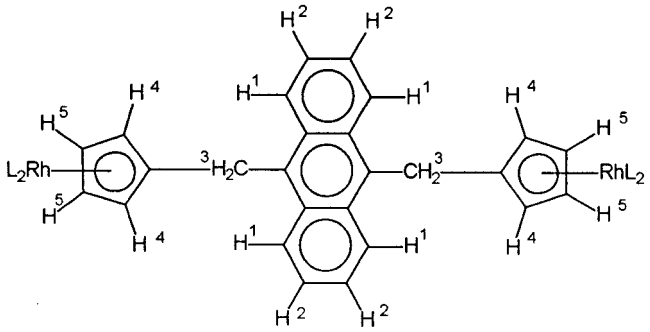

complex	δ (ppm), J/Hz
[(η^2-C_2H_4)$_2$Rh{$C_5H_4CH_2$(9,10-anthrylene)$CH_2C_5H_4$}Rh(η^2-C_2H_4)$_2$], **4**	8.52−8.42 (4 H, m, H^1), 7.40−7.28 (4 H, m, H^2), 4.70 (4 H, d, J_{HH} 4, H^5), 4.59 (4 H, d, J_{HH} 4, H^4), 4.47 (4 H, s, H^3), 2.79−2.58 (8 H, m, C_2H_4), 1.28−1.02 (4 H, m, C_2H_4)
[$(CO)_2$Rh{$C_5H_4CH_2$(9,10-anthrylene)$CH_2C_5H_4$}Rh$(CO)_2$], **5**	8.27−8.12 (4 H, m, H^1), 7.40−7.28 (4 H, m, H^2), 4.91 (4 H, d, J_{HH} 2, H^5), 4.71 (4 H, d, J_{HH} 2, H^4), 4.34 (4 H, s, H^3)
[(η^4-C_7H_8)Rh{$C_5H_4CH_2$(9,10-anthrylene)$CH_2C_5H_4$}Rh(η^4-C_7H_8)], **6**	8.29−8.20 (4 H, m, H^1), 7.22−7.13 (4 H, m, H^2), 4.91 (8 H, bs, H^4 and H^5), 4.55 (4 H, s, H^3), 2.79−2.58 (8 H, m, C_2H_4), 1.28−1.02 (4 H, m, C_2H_4), 2.98-2.91 (8 H, m, C_7H_8 vinylic protons), 3.07−3.01 (4 H, m, C_7H_8 allylic protons), 0.88 (4 H, t, J_{HH} 2, C_7H_8 methylene protons)

[a] Spectra recorded in C_6D_6; s = singlet; m = multiplet; d = doublet; bs = broad signal.

well-resolved ^{1}H NMR were obtained in C_6D_6 (Table 2) that are consistent with the proposed structures. Moreover, the observed spectral pattern is in agreement with that shown by several rhodium(I) complexes carrying a monosubstituted η^5-C_5H_4X ligand.[9,12] However, the resonance of the cyclopentadienylic and olefinic protons, in the case of both several monoanthryl-substituted rhodium(I) derivatives[9] and complexes **4**−**6**, is generally observed at a slightly higher field if compared with the corresponding η^5-C_5H_5 derivatives. Finally, it is interesting to note that the C−O infrared stretching frequencies of complex **5** (2042 and 1979 cm^{-1}), which are identical to those observed for (η^5-9-anthrylmethylcyclopentadienyl)dicarbonylrhodium(I),[9] are slightly lower than those exhibited by [Rh(η^5-C_5H_5)$(CO)_2$][13] (2051 and 1987 cm^{-1}), thus showing a moderately higher electron-donating power for the anthryl-substituted cyclopentadienyl ligands.

Attempts to obtain significant mass spectra for complexes **4**−**6** by conventional EI-MS or electronspray-MS techniques failed. Instead, interesting results were obtained by using a particle beam (PB) LC/MS system.[14] PB mass spectra were obtained in EI, positive-ion (PI), and negative-ion (NI) chemical ionization (CI) modes. Under EI conditions, the molecular ion was detected only for **6** (*m*/*z* 722, 30%). The subsequent loss of one or two ancillary ligands (η^4-C_7H_8) leads to the formation of the fragments at *m*/*z* 628 and 534, respectively. The most intense signal (*m*/*z* 436) is due to a fragment that arises from the loss of the two ancillary ligands, one rhodium center, and one hydrogen atom. Valuable spectral data were also obtained under PCI and NCI conditions. The PCI mass spectrum of **6** shows the protonated molecular ion as the most abundant signal. Peaks at *m*/*z* 628, 529, and 358 are attributable to the $[M - L - 2H]^+$, $[M - L - Rh + 2H]^+$, and $[M - 2L - RhCH(\eta^5\text{-}C_5H_4)]^+$ fragments, respectively. Instead, the NCI mass spectrum of this complex is mainly characterized by the peak at *m*/*z* 526 due to the release of one ancillary ligand, one rhodium center, and one hydrogen atom. In the case of compound **4**, the molecular ion peak could not be detected either in EI or in CI conditions. In its EI spectrum, the highest-mass fragment ion is observed at *m*/*z* 538, which arises from the loss of four ethylene ligands. This behavior is in agreement with the aforementioned lower thermal stability of **4** if compared with that of **5** and **6**. The spectrum of **4** shows also a signal at *m*/*z* 358, which is attributable to the $[M - 4L - RhCH(\eta^5\text{-}C_5H_4)]^+$ fragment ion. PCI ionization did not prove to be adequate for the analysis of **4** since a very low abundance-signal was obtained by the PB-MS system. Under NCI conditions, the elimination of three ethylene ligands is the most favored process, thus leading to the fragment at *m*/*z* 566 (base peak). As far as **5** is concerned, the highest-mass ions observed in its EI spectrum arise from the progressive loss of the carbonyl ligands from the molecular ion ($[M - 2CO]^+$, *m*/*z* 594, 3%; $[M - 4CO]^+$, *m*/*z* 538, 60%), the base-peak (*m*/*z* 435) being that attributable to the $[M - 4CO - Rh]^+$ ion, which arises from the loss of one rhodium center from the decarbonylated complex. Subsequent release of the CH(η^5-C_5H_4) moiety leads to the formation of the peak at *m*/*z* 358. Analogously, the decarbonylation pathway is favored under PCI conditions, as evidenced by the presence of the ions at *m*/*z* 539 ($[M - 4CO + H]^+$), *m*/*z* 567 ($[M - 3CO + H]^+$), *m*/*z* 595 ($[M - 2CO + H]^+$), and *m*/*z* 623 ($[M - CO + H]^+$). The peaks at *m*/*z* 359 and 437 are attributable to the [M − 4CO −

(12) (a) Arthurs, M.; Nelson, S. M.; Drew, M. G. B. *J. Chem. Soc., Dalton Trans.* **1977**, 779. (b) Diversi, P.; Ermini, L.; Ingrosso, G.; Lucherini, A. *J. Organomet. Chem.* **1993**, *447*, 291.

(13) Fischer, E. O.; Fischer, R. D. *Z. Naturforsch. B* **1961**, *16*, 475.

(14) (a) Careri, M.; Mangia, A.; Manini, P.; Predieri, G.; Sappa, E. *J. Organomet. Chem.* **1994**, *476*, 127. (b) Careri, M.; Mangia, A.; Manini, P.; Predieri, G.; Licandro, E.; Papagni, A. *Rapid Commun. Mass Spectrom.* **1997**, *11*, 51. (c) Careri, M.; Graiff, C.; Mangia, A.; Manini, P.; Predieri, G. *Rapid Commun. Mass Spectrom.* **1998**, *12*, 225.

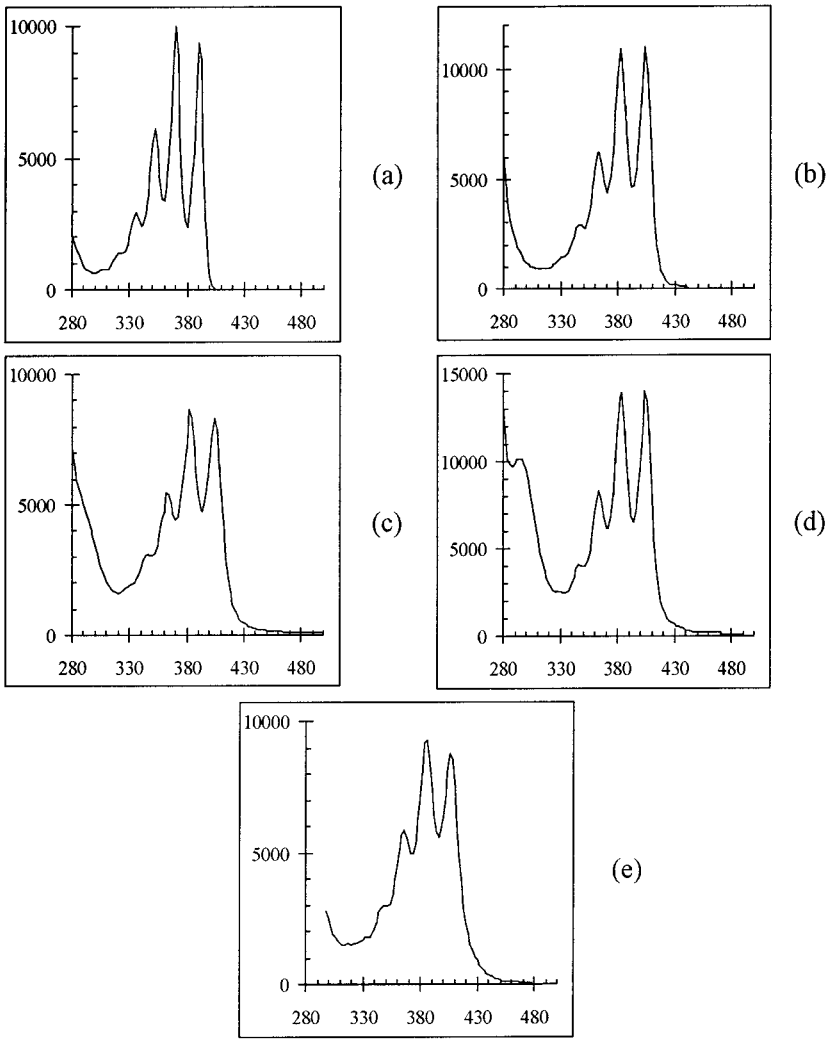

Figure 1. Absorption spectra (ϵ vs λ, nm) of 9-methylanthracene (a); 9,10-bis(cyclopentadienylmethyl)anthracene, **1** (b); [(η^2-C_2H_4)$_2$Rh{$C_5H_4CH_2$(9,10-anthrylene)$CH_2C_5H_4$}Rh(η^2-C_2H_4)$_2$], **4** (c); [(CO)$_2$Rh{$C_5H_4CH_2$(9,10-anthrylene)$CH_2C_5H_4$}-Rh(CO)$_2$], **5** (d); and [(η^4-C_7H_8)Rh{$C_5H_4CH_2$(9,10-anthrylene)$CH_2C_5H_4$}Rh(η^4-C_7H_8)] **6**, (e). All spectra were recorded in 5 $\times$ 10^{-5} to 10^{-4} M benzene solutions.

Table 3. Absorption Spectra and Fluorescence Data for 9,10-Bis(cyclopentadienylmethyl)anthracene, 1, Complexes 4−6, and Comparison with Those of 9-Methylanthracene and the Corresponding Monometallic Derivatives[a]

	absorption			fluorescence	
compound	λ_1	ϵ_1	$\epsilon_1/\epsilon_{min}$	λ_{max}	I_{rel}
9-methylanthracene	390	9600	3.96	391	100
9-anthrylmethylcyclopentadiene, **3**	392	12000	3.14	392	73
9,10-bis(cyclopentadienylmethyl)anthracene, **1**	404	11000	2.39	412	90
[Rh(η^5-$AnCH_2C_5H_4$)(η^2-C_2H_4)$_2$][b,c]	393	9000	2.19	393	0.3
[(η^2-C_2H_4)$_2$Rh{$C_5H_4CH_2$(9,10-anthrylene)$CH_2C_5H_4$}Rh(η^2-C_2H_4)$_2$], **4**	404	8500	1.78	413	6
[Rh(η^5-$AnCH_2C_5H_4$)(CO)$_2$][b,c]	392	10000	2.93	392	1.7
[(CO)$_2$Rh{$C_5H_4CH_2$(9,10-anthrylene)$CH_2C_5H_4$}Rh(CO)$_2$], **5**	404	14000	2.15	411	3
[Rh(η^5-$AnCH_2C_5H_4$)(η^4-C_7H_8)][b,c]	393	9200	1.84	393	8.7
[(η^4-C_7H_8)Rh{$C_5H_4CH_2$(9,10-anthrylene)$CH_2C_5H_4$}Rh(η^4-C_7H_8)], **6**	406	8800	1.57	412	15

[a] All spectra were recorded in benzene solution. [b] $AnCH_2C_5H_4$ = 9-anthrylmethylcyclopentadienyl ligand; λ are in nm; ϵ is given as M^{-1} cm^{-1}. [c] Ref 9.

RhCH(η^5-C_5H_4) + H]$^+$) and [M − 4CO − Rh + H]$^+$), respectively. A different pattern characterizes the NCI mass spectrum of complex **5**. The formation of the molecular ion is evidenced by the peak at *m*/*z* 650 (6%), whereas the most intense signal at *m*/*z* 594 corresponds to the [M − 2CO]$^-$ fragment ion.

2.2. Absorption and Emission Spectroscopic Studies. The UV−visible spectra (280−800 nm) of complexes **4**−**6** along with those of 9-methylanthracene and 9,10-bis(cyclopentadienylmethyl)anthracene (**1**) are shown in Figure 1. The parameters of the last vibrational bands are compared with those of monosubstituted anthracene derivatives in Table 3.

Moreover, the UV−visible spectra of three reference complexes, i.e., [Rh(η^5-C_5H_5)(η^2-C_2H_4)$_2$], [Rh(η^5-C_5H_5)-(CO)$_2$], and [Rh(η^5-C_5H_5)(η^4-C_7H_8)], are reported in Figure 2, which shows that all these complexes have relatively small absorption coefficients above 330 nm.

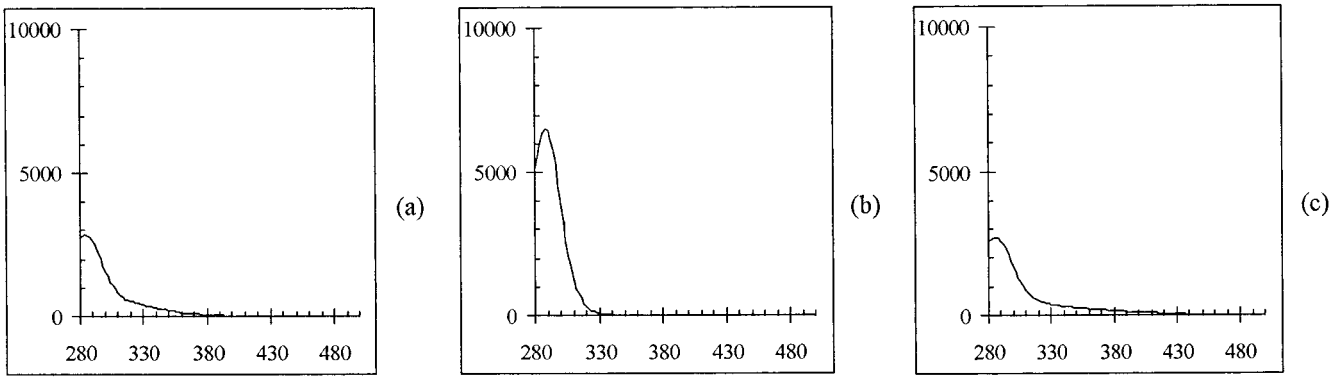

Figure 2. Absorption spectra (ϵ vs λ, nm) of [Rh(η^5-C_5H_5)(η^2-C_2H_4)$_2$] (a); [Rh(η^5-C_5H_5)(CO)$_2$] (b); and [Rh(η^5-C_5H_5)(η^4-C_7H_8)] (c). All spectra were recorded in 5×10^{-5} to 10^{-4} M benzene solutions.

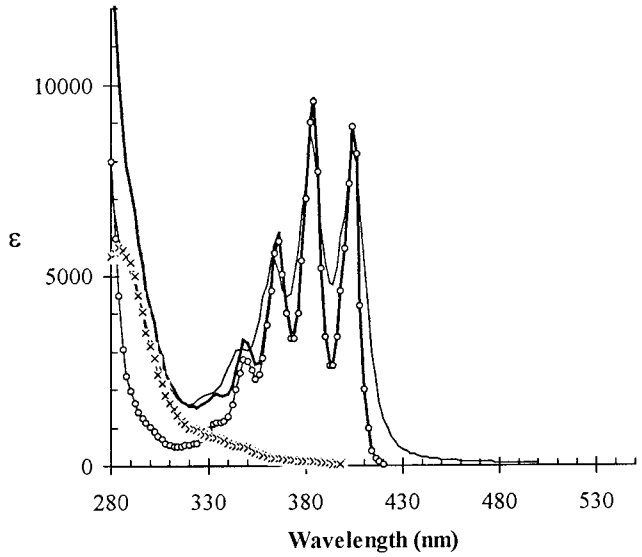

Figure 3. Comparison of the UV−visible spectrum of [(η^2-C_2H_4)$_2$Rh{$C_5H_4CH_2$(9,10-anthrylene)$CH_2C_5H_4$}Rh(η^2-C_2H_4)$_2$], **4** (−), with the sum (—) of the spectra of 9-methylanthracene (∘-∘-∘-∘) and of [Rh(η^5-C_5H_5)(η^2-C_2H_4)$_2$] (×-×-×).

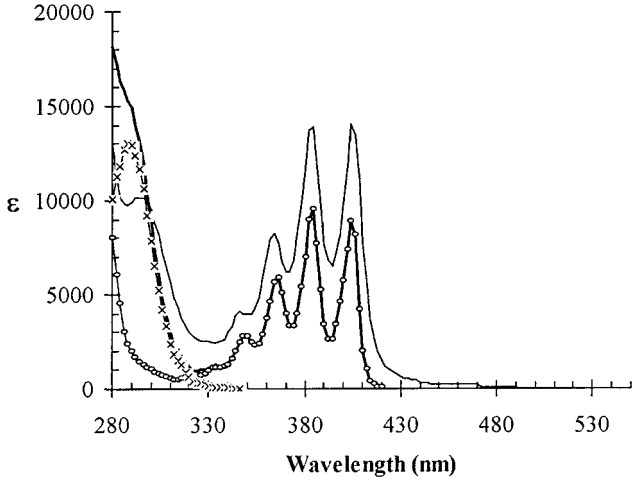

Figure 4. Comparison of the UV−visible spectrum of [(CO)$_2$Rh{$C_5H_4CH_2$(9,10-anthrylene)$CH_2C_5H_4$}Rh(CO)$_2$], **5** (−), with the sum (—) of the spectra of 9-methylanthracene (∘-∘-∘) and of [Rh(η^5-C_5H_5)(CO)$_2$] (×-×-×).

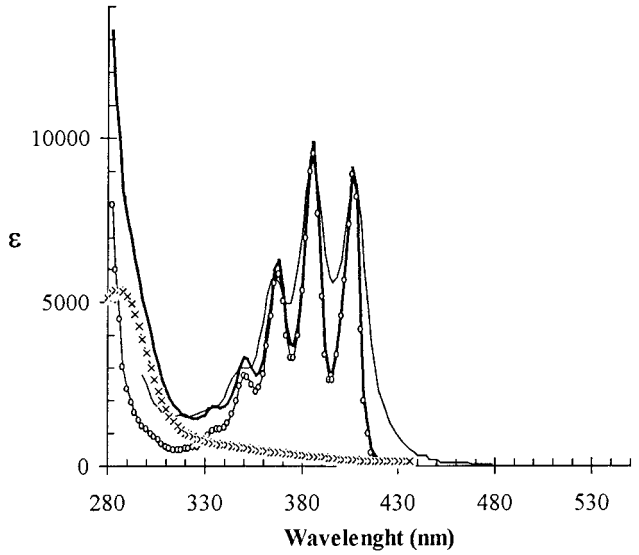

Figure 5. Comparison of the UV−visible spectrum of [(η^4-C_7H_8)Rh{$C_5H_4CH_2$(9,10-anthrylene)$CH_2C_5H_4$}Rh(η^4-C_7H_8)], **6** (−), with the sum (—) of the spectra of 9-methylanthracene (∘-∘-∘) and of [Rh(η^5-C_5H_5)(η^4-C_7H_8)] (×-×-×).

With one exception, i.e., the relatively higher molar absorption coefficient of **5**, which was verified by successive purification of the analytical sample, the absorption spectra of the 9,10-disubstituted anthracene derivatives are typical of the anthracene moiety, when a bathochromic shift of ca. 12 nm of the maxima is included, so that all the substituents can be treated as perturbations of the anthracene chromophore. Furthermore, the substitution at the carbon atoms 9 and 10 with identical groups causes a decrease in the spectral resolution compared with the one exhibited in the spectra of the monosubstituted anthracene derivatives (Table 3). This is a quite unexpected observation. In fact, the second substitution causes an increase in the apparent molecular symmetry so that a smaller number of vibrations play a role in the absorption spectrum, which should result in an increase of spectral resolution. The second observation to be accounted for is the presence of a long-wavelength tail (above 430 nm), which becomes evident when the spectra of the complexes **4**−**6** are compared with those obtained by adding the spectra of the model compounds, i.e. [Rh(η^5-C_5H_5)(η^2-C_2H_4)$_2$], [Rh(η^5-C_5H_5)(CO)$_2$], and [Rh(η^5-C_5H_5)(η^4-C_7H_8)], to that of 9-methylanthracene after a shift of ca. 14 nm (Figures 3−5).

Insight into the spectral properties of **4**−**6** may be gained by looking at these complexes as molecular

entities constituted of subunits, i.e., the anthracene fragment and the cyclopentadienylRhL$_2$ moiety, acting as electron-acceptor or electron-donor groups, as was substantiated by electrochemical studies (section 2.3). Accordingly, two complementary interpretations of the above observations can be suggested. The first stems from the fact that the presence of the methylene spacer, which links the subunits, allows an infinite number of conformations for **4**−**6**. Since it is highly plausible that the strength of the electronic interaction between the subunits changes with variation in the molecular geometry, the energies of the absorption bands of the various conformers should be different and thus produce some spectral broadening. Moreover, poorly populated conformations having low energy could be responsible for the observed tail. The other possible interpretation is that the lowest electronic transition is due to an intramolecular charge transfer and thus is weak, so that the observed structured transitions would be less resolved, being coupled to a lower lying excited state. Finally, the relatively high molar absorption coefficient exhibited by **5** is at least partially explained by its increased spectral resolution.

The fluorescence properties of complexes **4**−**6** were explored by using the Rayleigh scattering peak as an internal reference to measure the relative fluorescence intensity, as previously reported.[9] While the cyclopentadienyl complexes [Rh(η^5-C_5H_5)(η^2-C_2H_4)$_2$], [Rh(η^5-C_5H_5)(CO)$_2$], and [Rh(η^5-C_5H_5)(η^4-C_7H_8)] as well as the mono(9-anthrylmethyl)cyclopentadienyl derivatives, [Rh(η^5-AnCH$_2$C$_5$H$_4$)L$_2$] (An = 9-anthryl),[9] do not exhibit any measurable emission, **4**−**6** have relatively high emission intensities, but much lower than those observed for 9-methylanthracene, 9-anthrylmethylcyclopentadiene, and 9,10-bis(cyclopentadienylmethyl)anthracene (**1**) (Table 3). Even if poorly resolved, the fluorescence spectra of **4**−**6** are typical of the anthracene fluorophore, with the first maximum occurring at ca. 412 nm. Since all the studied compounds show high purity on chemical analysis, it is quite unlikely that the observed fluorescence emission was due to an anthracene-based impurity. It should be noted that the shift between the absorption and the fluorescence spectra, which is almost negligible in the case of the mono(9-anthrylmethy)cyclopentadienyl derivatives,[9] is quite large (ca. 9 nm) in the case of **1** and **4**−**6** in a nonpolar solvent (Table 3). Finally, it must be pointed out that **1** and **4**−**6** have similar absorption and fluorescence spectra, but their fluorescence emission intensities are quite different. Thus, it seems that the presence of the rhodium centers does not appear to influence the energy levels of the anthracenic fluorophore but rather to reduce the emission probability, by increasing the spin−orbit coupling, and thus to increase the intersystem crossing.

As discussed above, an infinite number of molecular conformations are possible for complexes **4**−**6**, but conformations that allow a rather strong interaction between the subunits are not expected to be favored in the ground state since closed shell orbitals are involved. In the excited state, the two substituents being identical, the electronic delocalization on both the cyclopentadienylRhL$_2$ subunits will instead reduce the overall energy. To allow the electronic energy to be spread on

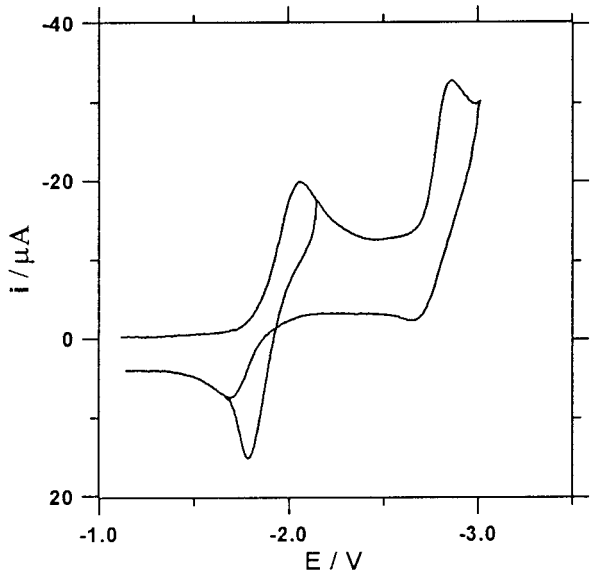

Figure 6. Cyclic voltammetric curve of a 2.0 mM THF solution of **4** in the presence of TBAPF$_6$ (0.05 M). T = 25 °C, ν = 0.5 V/s, working electrode: platinum.

the cyclopentadienylRhL$_2$ moieties, a significant reorganization of the molecular geometry must occur after excitation, as often observed. This could explain the observed shift between the absorption and the fluorescence spectra. Moreover, since fluorescence intensity is relatively high in **4**−**6**, the lowest excited state must receive a fairly large contribution from the anthracene. Because state coupling depends on the energy difference between the electronic states involved, the contribution of anthracene to the lower electronic excited state would be expected to decrease along the series **6** > **4** > **5**. There is indeed a direct correlation between the absorption tail (Figure 2) and the fluorescence emission intensity (Table 3) of such complexes:

	5	**4**	**6**
upper limit of the absorption tail	330 nm	380 nm	430 nm
fluorescence intensity	3%	6%	15%

2.3. Electrochemical Studies. The CV curve for a 2.0 mM THF solution of **4** is shown in Figure 6. Two reduction peaks are observed: both reductions are monoelectronic, the first one reversible ($E_{1/2}$ = −1.87 V) and the second irreversible (E_p = −2.87 V). The reversibility of the first peak is greatly affected by the occurrence of the second reduction. The morphology of the curve is similar to that found for analogous monometallic complexes[9] and shows that the cyclopentadienylRhL$_2$ moiety is not involved in the reduction processes, which are therefore localized on the 9,10-anthrylenic unit. The increased separation between the two reduction processes, compared with that found in the monometallic complexes and in 9-anthrylmethylcyclopentadiene,[9] may result from an increased electronic coupling interaction due, in the bimetallic species, to the double substitution of the anthrylic moiety. No oxidation processes were observed, probably due to the narrow anodic potential window available in the present solvent.

Figure 7 shows the CV curve for a 1.0 mM THF solution of **6**. Again two reduction processes are ob-

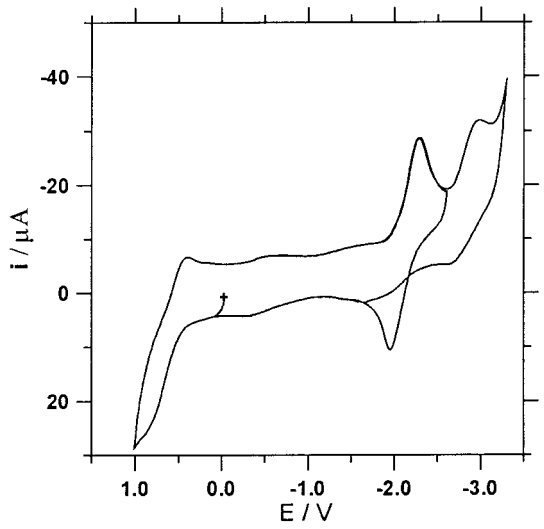

Figure 7. Cyclic voltammetric curve of a 1.0 mM THF solution of **6** in the presence of $TBAPF_6$ (0.05 M). $T = 26$ °C, $v = 0.5$ V/s, working electrode: platinum.

served. The first reduction is reversible ($E_{1/2} = -1.98$ V) only when the second peak, that is only partially reversible, is not included in the CV scan. The potentials at which the two reductions take place are quite close to those found for **4** and are likewise attributed to the first and the second reduction of the 9,10-anthrylenic unit. At odds with **4**, an oxidation process for **6** was observed, with $E_{1/2} = 0.75$ V (Figure 7).

The presence of a cathodic counterpart of such a peak indicates that the oxidation is reversible, and, by comparison with the reduction peaks, it corresponds to the exchange of one electron. This might indicate that, analogously to the reduction processes, the oxidation involves also the 9,10-anthrylenic unit. However, the absence of any oxidation peaks in the CV curve of **4** (and likewise in that of **5**, vide infra), under the present conditions, suggests that the occurrence of such a process could depend on the nature of the ancillary ligands L of the cyclopentadienylRhL_2 moieties. Therefore, one could infer that such a process involves the oxidation of the latter units. In the case of **6**, L_2 = norbornadiene, the stronger electron-donating properties of the ligand if compared with ethylene and carbon monoxide (vide infra) would in fact allow the oxidation to be observed before the occurrence of the solvent/electrolyte discharge. It must be noted that only one electron is involved in the oxidation process, while, in view of the equivalency of the two cyclopentadienylRhL_2 moieties, one could expect the exchange of two electrons. This result may be explained assuming a significant interaction between the two metal-containing units which would make the two oxidations occur at different potentials. The observed process would then lead to the mixed-valence [Rh^{+1}, Rh^{+2}] compound, and the second oxidation would not be observed, under the present conditions, because it occurs outside of the available anodic potential window. Alternatively, if the redox orbital involved in the oxidation process is largely delocalized over the two cyclopentadienylRhL_2 moieties, then the oxidation process would lead to a species where the two metals have an average +1.5 redox state. **5** exhibits a CV behavior quite similar to those found in the case of **4** and **6**. Again, a reversible reduction ($E_{1/2}$ = −1.94 V) and an irreversible peak ($E_p = -2.90$ V) are observed, both being localized onto the 9,10-anthrylenic moiety and, similarly to **4**, no oxidation process was observed, under the same experimental conditions.

Table 4. Electrochemical Data for Complexes 4−6[a]

complex	oxidations	reductions
4	0.44[c,d]	−1.87[b]/−2.87[c]
5	0.82[c,d]	−1.94[b]/−2.90[c]
6	0.37[c,d]/0.75[b]	−1.98[b]/−2.80[c]

[a] V vs SCE, $T = 25$ °C; working electrode: Pt, THF/$TBAPF_6$ unless otherwise stated. [b] $E_{1/2}$. [c] E_p (irreversible peak, at 0.5 V/s). [d] CH_3CN/$TBAPF_6$.

Complementary CV experiments were carried out in CH_3CN in order to obtain further information about the behavior of complexes **4**−**6** under oxidation conditions.[16] This solvent, in fact, allows a wider anodic potential window than THF. Indeed, an irreversible anodic oxidation peak was observed for all the species, with a positive peak potential which increases in the series **6** (L_2 = norbornadiene) < **4** (L = ethylene) < **5** (L = CO) (Table 4).

A reversible CV pattern was not obtained under the adopted conditions and at scan rates as high as 20 V/s. The peak potential shifted anodically by ca. 30 mV/decade for all the species. This is consistent with an EC (electrochemical-chemical) mechanism, i.e. with the occurrence of a follow-up fast chemical reaction responsible for the observed irreversibility. Assuming a similar value for the rate constant of such a reaction for **4**−**6**, the peak potentials, as measured under the same conditions, should reflect the differences among the respective standard potentials. The observed trend would then indicate that the oxidation process involves, in all the species, the cyclopentadienylRhL_2 moieties, since the stronger the electron-donor properties of the ancillary ligands L, the easier the oxidation is. This is in line with what was anticipated above, on the basis of the electrochemical behavior of **4**−**6** in THF, and also with the electrochemical properties of the parent mononuclear compounds, elsewhere reported.[17] Owing to (i) such a localization of the oxidation process, (ii) the fact that it involves the exchange of a single electron, and, finally, (iii) that no other oxidation processes were observed at more positive potentials within several hundred millivolts (as expected for two equivalent and weakly interacting redox sites), an average-valence (+1.5) compound is proposed for the species arising from the one-electron oxidation of complexes **4**−**6**.

The occurrence of an intramolecular charge-transfer process between the photoexcited 9,10-anthrylenic moiety and the cyclopentadienylRhL_2 units is a possible route for the observed quenching of emission in **4**−**6**. This hypothesis is subject to the thermodynamic requirement that the resulting charge-separated state is exoergonic with respect to the anthracene-based excited state. The driving force for the process may in fact be

(15) Jons, R. N. *J. Am. Chem. Soc.* **1945**, *67*, 2127.

(16) CV experiments were also carried out in CH_2Cl_2 in order to obtain information relative to radical cations **4**−**6** under conditions similar to those used in EPR experiments. However, in that medium, the oxidative pattern was severely disturbed by adsorption phenomena, involving the oxidated species, which made the analysis of the CV curves unfeasible.

(17) Cicogna, F.; Ingrosso, G.; Pinzino, C.; Roffia, S. et al. To be submitted.

calculated from the electrochemical and spectroscopic (emission) data by using the equation $-\Delta G_{cs} = E_{0-0} - (E°_D - E°_A) - \Delta G_s$, where E_{0-0} (3.2 eV) is the 0−0 energy of the anthracene-based excited state, estimated from the emission maximum in the model, i.e., 9-methylanthracene; $E°_D$ and $E°_A$ are the standard potentials for the oxidation of the donor, i.e., cyclopentadienylRhL$_2$ moieties, and the reduction of the acceptor, i.e., the 9,10-anthrylenic moiety, respectively, and ΔG_s is the correction term for the effects of ion−solvent interaction for the charge-separated (D^+-A^-) species. The reversible data obtained in THF for **6** allow the evaluation of ΔG_{cs}: although not including the stabilization effect for ion−solvent interaction (ΔG_s), the reductive quenching process is, in this case, highly exoergonic ($-\Delta G_{cs} = 0.47$ eV) and therefore represents a possible mechanism for the quenching of the anthrylenic unit emission. By contrast, the E_p values obtained for **4**−**6** in CH_3CN cannot be used for an accurate evaluation of the respective ΔG_{cs}. The follow-up reactions, coupled to the oxidation processes, bring about a negative shift of the CV peaks with respect to the reversible case. Thus, the driving forces, calculated on the basis of such peak potentials, are therefore necessarily overestimated. Taking into account these limitations and considering the large excess energy of the starting excited state (3.2 eV) as well as the stabilization due to the interaction of the charge-separated state with the solvent, the data of Table 4 would however indicate that also for **4** and **5** the intramolecular reductive quenching process is a viable route.

2.4. Chemical Oxidation of Complexes 4−6: EPR Studies and DFT Calculations. A preliminary investigation on the chemical oxidation of complexes **4**−**6** led us to use successfully thallium(III) trifluoroacetate as the oxidant in a 1:1 dichloromethane/1,1,1,3,3,3-hexafluoropropan-2-ol mixture, the latter being a superior solvent for the generation and stabilization of radical cations.[18] Following an already described procedure,[19] reactants were made to come into contact at low temperature (−80 °C) in the cavity of the EPR spectrometer, and then the temperature was gradually raised until a signal appeared. In the case of the complex [(CO)$_2$Rh{C$_5$H$_4$CH$_2$(9,10-anthrylene)CH$_2$C$_5$H$_4$}Rh(CO)$_2$] (**5**), no signal appeared at temperatures lower than −5 °C. At this temperature, a well-resolved spectrum ($g_{iso} = 2.0055$; $\Delta H_{pp} = 0.51$ G) is obtained (Figure 8) that is consistent with a radical cation exhibiting a spin delocalization confined mainly to two rhodium centers ($I = 1/2$) ($a_{Rh} = 23.47$ G, 2 Rh) and to four sets of protons ($a^1_H = 11.64$ G, 2 H; $a^2_H = 6.29$ G, 2 H; $a^3_H = 5.88$ G, 1 H; $a^4_H = 2.94$ G, 1 H). The hyperfine coupling constants and line-widths were obtained by computer simulation of the experimental spectrum.

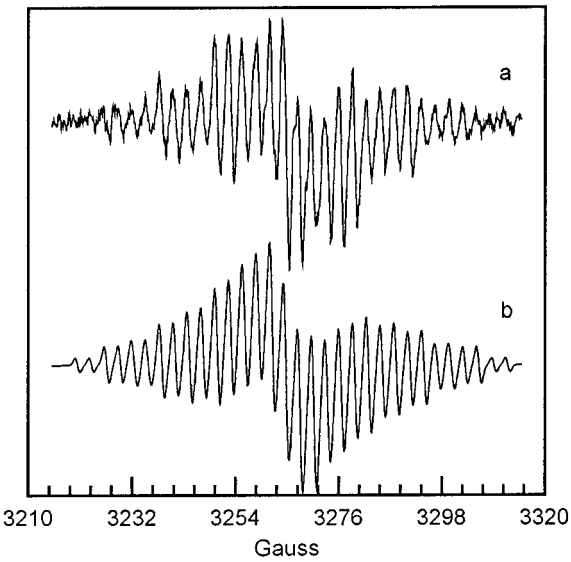

Figure 8. Experimental (a) and simulated (b) EPR (X-band) spectra of the radical cation **5**$^+$; $T = 268$ K; $g_{iso} = 2.0055$; $\Delta H_{pp} = 0.51$ G.

Within ca. 30 min, at 0 °C, this radical species is transformed into a new one in which, according to its EPR spectrum ($g_{iso} = 2.0060$; $\Delta H_{pp} = 0.36$ G) (Figure 9), the spin delocalization extends over the whole 9,10-bis(cyclopentadienylmethyl)anthracene skeleton with a lower isotropic hyperfine splitting to the metal centers ($a_{Rh} = 5.29$ G, 2 Rh; $a^1_H = 2.15$ G, 2 H; $a^2_H = 2.44$ G, 2 H; $a^3_H = 2.56$ G, 2 H; $a^4_H = 2.14$ G, 2 H; $a^5_H = 3.85$ G, 4 H; $a^6_H = 1.03$ G, 4 H). At 0 °C, this species is kinetically very stable, showing a lifetime of ca. 1.5 h.

The EPR spectra of Figures 8 and 9 can be associated with two radical species having the same skeletal structure, i.e., that of the cation radical **5**$^+$, but different conformations and very different spin delocalization. Expectedly, the spin distribution over a given molecular skeleton is extremely sensitive to even small geometrical changes.[20]

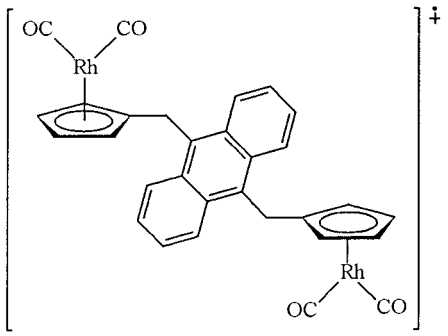

5$^+$

When [(η^2-C$_2$H$_4$)$_2$Rh{C$_5$H$_4$CH$_2$(9,10-anthrylene)CH$_2$C$_5$H$_4$}Rh(η^2-C$_2$H$_4$)$_2$] (**4**) was reacted with thallium(III) trifluoroacetate, we succeeded in detecting only one radical species, at 0 °C, exhibiting the well-resolved EPR spectrum ($g_{iso} = 2.0059$; $\Delta H_{pp} = 0.36$ G) shown in the Figure 10. Such a spectrum is extremely similar to the spectrum of Figure 9 and can be associated with the

(18) (a) Eberson, L.; Hartshorn, M. P.; Persson, O. *J. Chem. Soc., Perkin Trans.* **1995**, 1735. (b) Eberson, L.; Hartshorn, M. P.; Persson, O.; Radner, F. *J. Chem. Soc., Chem. Commun.* **1996**, 2105.

(19) (a) Diversi, P.; Forte, C.; Franceschi, M.; Ingrosso, G.; Lucherini, A.; Petri, M.; Pinzino, C. *J. Chem. Soc., Chem. Commun.* **1992**, 1345. (b) Bruni, M.; Diversi, P.; Ingrosso, G.; Lucherini, A.; Pinzino, C.; Raffaelli, A. *J. Chem. Soc., Dalton Trans.* **1995**, 1035. (c) Diversi, P.; Iacoponi, S.; Ingrosso, G.; Laschi, F.; Lucherini, A.; Pinzino, C.; Uccello-Barretta, G.; Zanello, P. *Organometallics* **1995**, *14*, 3275. (d) Bruni, M.; Diversi, P.; Ingrosso, G.; Lucherini, A.; Pinzino, C. *Gazz. Chim. Ital.* **1996**, *126*, 239. (e) Diversi, P.; Ferrarini, A.; Ingrosso, G.; Lucherini, A.; Uccello-Barretta, G.; Pinzino, C.; De Biani Fabrizi, F.; Laschi, F.; Zanello, P. *Gazz. Chim. Ital.* **1996**, *126*, 391.

(20) Pople, J. A.; Beveridge, D. L. *Approximate Molecular Orbital Theory*; McGraw-Hill: New York, 1970.

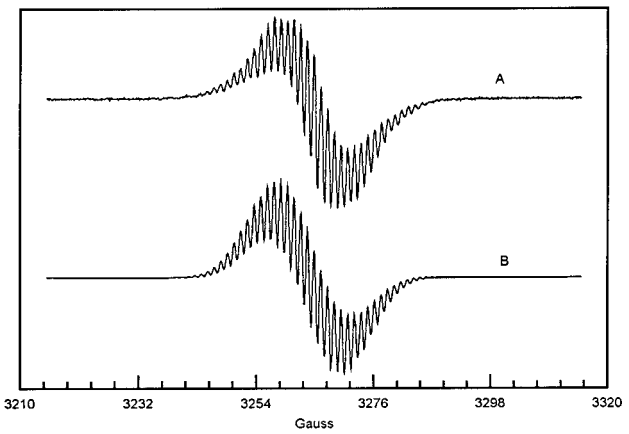

Figure 9. Experimental (A) and simulated (B) EPR (X-band) spectra of the radical cation $\mathbf{5}^+$ (evolution); $T = 273$K; $g_{iso} = 2.0060$; $\Delta H_{pp} = 0.36$ G.

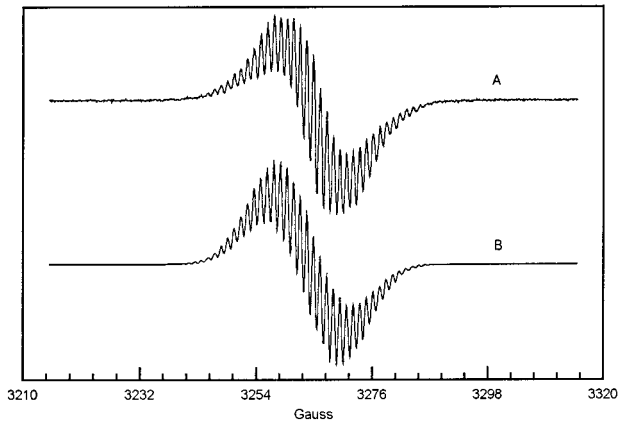

Figure 10. Experimental (A) and simulated (B) EPR (X-band) spectra of the radical cation $\mathbf{4}^+$; $T = 273$ K; $g_{iso} = 2.0059$; $\Delta H_{pp} = 0.36$ G.

cation radical $\mathbf{4}^+$, which again is a kinetically stable species. Indeed, computer simulation of the spectrum shows again that the spin delocalization extends over the anthracene system, the methylene groups, the cyclopentadienyl ligands, and the metal centers ($a_{Rh} = 5.25$ G, 2 Rh; $a^1_H = 2.20$ G, 2 H; $a^2_H = 2.14$ G, 2 H; $a^3_H = 2.42$ G, 2 H; $a^4_H = 2.14$ G, 2 H; $a^5_H = 3.89$ G, 4 H; $a^6_H = 1.00$ G, 4 H).

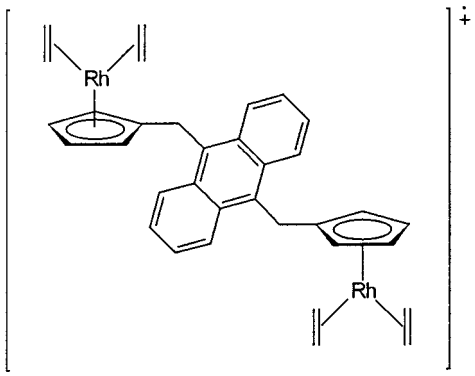

$\mathbf{4}^+$

The oxidation of the norbornadiene derivative [(η^4-C_7H_8)Rh{$C_5H_4CH_2$(9,10-anthrylene)$CH_2C_5H_4$}Rh(η^4-C_7H_8)] (**6**) with thallium(III) trifluoroacetate led to less satisfactory results. Indeed, most probably because of the low solubility of the resulting products in the reaction medium, an intense one-line EPR spectrum was recorded, at 0 °C, without any hyperfine structure.

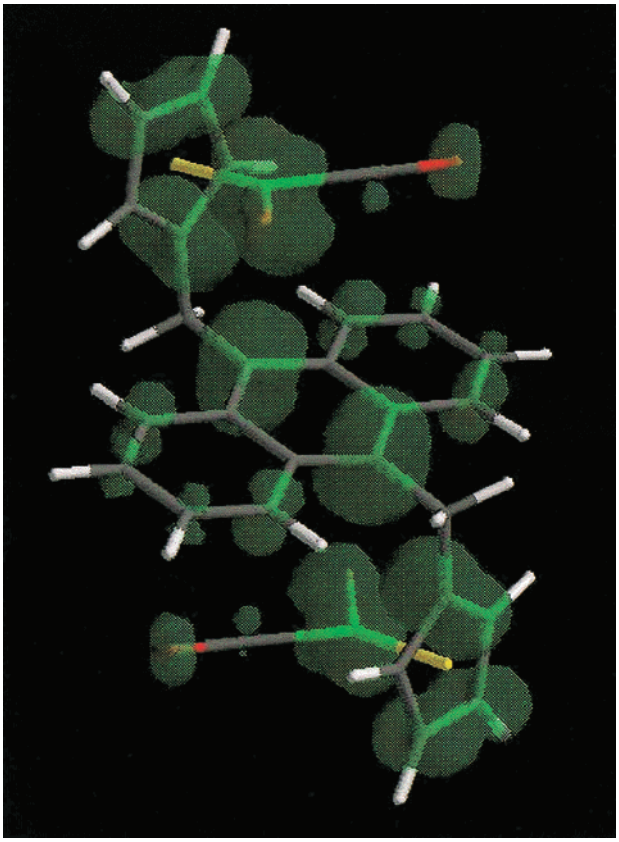

Figure 11. Spin density surface (0.002 electron/au^3) of the radical cation $\mathbf{5}^+$.

DFT calculation of the spin density distribution by using the Spartan 5.1.3. program (Model LSDA/pBP86/DN**)[21,22] allowed a theoretical evaluation of the isotropic hyperfine coupling constants for the various hydrogen atoms in the more stable species $\mathbf{4}^+$ and $\mathbf{5}^+$, also furnishing a further insight into the structure of such species. For the sake of clarity only the negative spin density is represented in the spin density maps reported in Figures 11 and 12. Anyway, the positive and negative spin density distribution shows clearly that, in the optimized geometry, the unpaired electron delocalizes over the whole molecular skeleton.

When comparing the theoretical and experimental isotropic hyperfine coupling constants, the limited basis set used, the influence of the solvent, and the vibrational and environmental effects should be take into account in the calculation to produce quite accurate results. Since it is hard to asses the importance of such effects, a semiempirical extrapolation procedure[23] has been adopted to correct the theoretical values and compare them with the experimental ones. Interestingly, the calculated isotropic hyperfine coupling constants for the cation radical $\mathbf{4}^+$ ($a_{H1} = a_{H4} = a_{H5} = a_{H8} = -2.3$ G; $a_{H2} = a_{H3} = a_{H6} = a_{H7} = -2.0$ G; $a_{H12} = a_{H13} = a_{H16} = a_{H17} = -3.8$ G; $a_{H9} = a_{H10} = 1.0$ G) (see hydrogen numbering

(21) Beche, A. D. *Phys. Rev. A* **1988**, *38*, 3098.
(22) Perdew, J. P. *Phys Rev. B* **1986**, *33*, 8822.
(23) (a) Fortunelli A.; Salvetti, O. *J. Mol. Struct. (THEOCHEM)* **1993**, *287*, 89. (b) Fortunelli, A. *Int. J. Quantum Chem.* **1994**, *52*, 97.

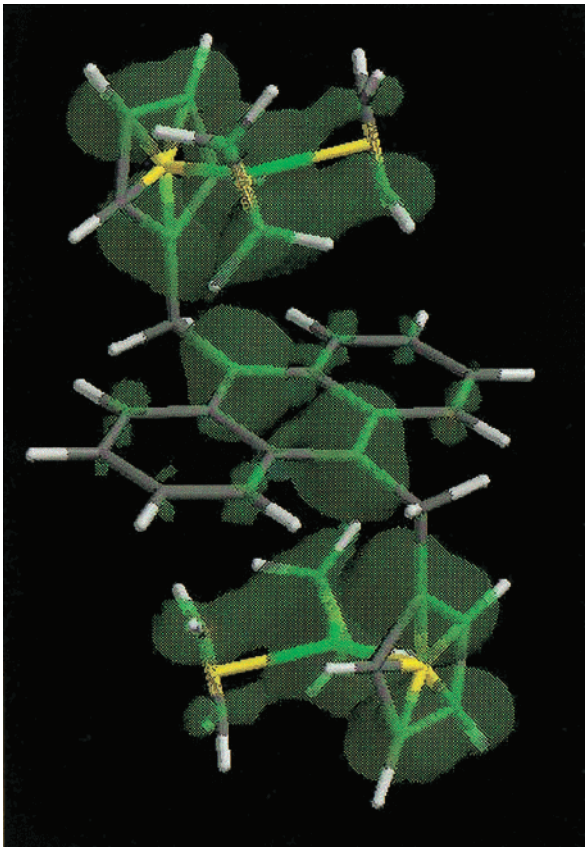

Figure 12. Spin density surface (0.002 electron/au^3) of the radical cation $\mathbf{4}^+$.

given below) and $\mathbf{5}^+$ ($a_{H1} = a_{H4} = a_{H5} = a_{H8} = -2.5$ G; $a_{H2} = a_{H3} = a_{H6} = a_{H7} = -2.1$ G; $a_{H12} = a_{H13} = a_{H16} = a_{H17} = -3.9$ G; $a_{H9} = a_{H10} = 1.1$ G) are in a remarkable accordance with those reported above, which were obtained by computer simulation of the experimental spectra of Figures 9 and 10, respectively.

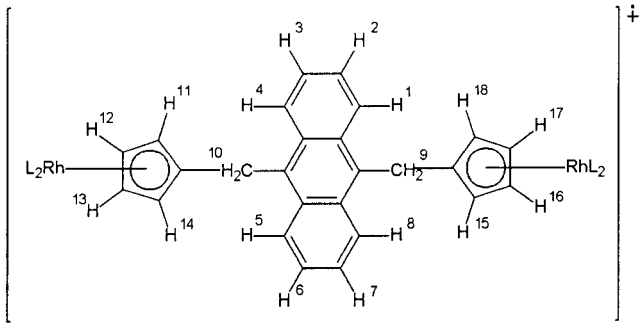

In conclusion, according to the EPR spectra and DFT calculations, the two metal centers of the cation radicals $\mathbf{4}^+$ and $\mathbf{5}^+$ are largely electronically coupled so that the odd electron of the mixed-valence state is evenly delocalized between the two metal centers, and the description of $\mathbf{4}^+$ and $\mathbf{5}^+$ as [Rh$^{+1/2}$, Rh$^{+1/2}$] complexes is more appropriate.

3. Concluding Remarks

In summary, we have shown that the UV−visible spectra of the homo-bimetallic anthracene-bridged η^5-cyclopentadienyl derivatives of rhodium(I) [$L_2Rh\{C_5H_4CH_2$(9,10-anthrylene)$CH_2C_5H_4\}RhL_2$] **4**−**6** are indicative of the existence of a strong electronic communication between the anthracenic bridging ligand and the two cyclopentadienylRhL_2 moieties. Furthermore, the EPR spectroscopy documents clearly that a long-range interaction exists between the two metal centers in the products, resulting from the one-electron oxidation of complexes **4**−**6**, i.e., the cation radicals [$L_2Rh\{C_5H_4CH_2$-(9,10-anthrylene)$CH_2C_5H_4\}RhL_2]^+$ $\mathbf{4}^+$−$\mathbf{6}^+$. This means that the d-electrons of the metal centers are in π-symmetry orbitals and can effectively overlap with the π-orbitals of the bridging fragment; therefore, they are delocalized to some extent across the connecting ligand. Accordingly, it has been shown by means of DFT calculation of the spin density distribution that, in the optimized geometry, the odd electron is delocalized over the whole metal−bridge−metal system. Thus, the cation radicals $\mathbf{4}^+$−$\mathbf{6}^+$, which on the basis of the EPR and electrochemical studies are best described as [Rh$^{+1/2}$, Rh$^{+1/2}$] complexes, appear to be interesting examples of "one-dimensional molecular wires". In the field of mixed-valence chemistry, compounds like these are usually said to show class III behavior,[24] and as such, they should not be called supramolecular species.[4] Finally, we have shown that while 9,10-bis(cyclopentadienylmethyl)anthracene (**1**) is an efficient light-emitting molecule, the fluorescence of the 9,10-anthrylene group is significantly quenched in the bimetallic derivatives **4**−**6** most probably due to the occurrence of an electron transfer from the cyclopentadienylRhL_2 moiety to the excited 9,10-anthrylene, a process that on the basis of the electrochemical data may be justified on thermodynamic grounds.

In conclusion, all the above points make the 9,10-bis(methylene)anthracene appear a promising bridging ligand for assembling potentially useful molecular devices since it, owing to its electronic and conformational properties, may switch on/off the communication between the linked sites.

4. Experimental Details

4.1. General Procedures. The reactions and manipulations of organometallics were carried out under dinitrogen or argon using standard techniques. All solvents were dried and distilled prior to use following standard procedures. Microanalyses were performed by the Laboratorio di Microanalisi, Facoltà di Farmacia, Università di Pisa. ^{1}H NMR spectra were run at 200 MHz on a Varian Gemini 200 instrument. Infrared spectra were obtained by a FT-IR Perkin-Elmer 1750 spectrometer. Electron ionization mass spectra (EI-MS) were obtained with a VG Analytical 7070E apparatus. The particle beam-mass spectrometry (PB-MS) analyses were performed on a Hewlett-Packard model 5989A mass spectrometer provided with a Hewlett-Packard model 59980A particle beam interface. The flow-injection (FIA) mode was used for sample introduction. Dichloromethane solutions of the complexes were injected using a Hewlett-Packard model 1090 HPLC pump; acetonitrile was used as the eluant at a flow-rate of 0.4 mL/min. The nebulizing gas for particle beam interface was high-purity helium (inlet pressure 40 psi); the temperature of the desolvation chamber was 40 °C. The mass spectrometer was equipped with a dual electron impact/chemical ionization (EI/CI) source, a hyperbolic mass analyzer, a continuous dinode electron multiplier detector, and a differentially pumped

(24) Robin, M. B.; Day, P. *Adv. Inorg. Chem. Radiochem.* **1967**, *10*, 247.

vacuum system with diffusion pumps. The Hewlett-Packard MS 59940 ChemStation (HP-UX series) was used as analytical workstation. Both EI and CI techniques were used: positive and negative ion CI mass spectra were obtained, with methane as the reagent gas. The source and the quadrupole temperatures were maintained at 250 and 100 °C, respectively; the ionization energy was 70 eV in the EI mode and 150 eV in the CI mode. The voltage applied to the electron multiplier was 2300 V; the system was scanned from 80 to 800 amu at a rate of 1.16 s per scan.

Cyclopentadienylsodium,[25] di-μ-chlorotetrakis(carbonyl)dirhodium(I),[26] di-μ-chlorotetrakis(η^2-ethylene)dirhodium(I),[27] di-μ-chlorobis(η^4-norbornadiene)di-rhodium(I),[28] (η^5-cyclopentadienyl)bis(η^2-ethylene)rhodium(I),[29] (η^5-cyclopentadienyl)dicarbonylrhodium(I),[13] and 9,10-bis(bromomethyl)anthracene[11] were prepared as reported. (η^5-Cyclopentadienyl)(η^4-norbornadiene)rhodium(I) was prepared according to described procedures.[30] Thallium(I) ethoxide (Aldrich), 9-methylanthracene (Aldrich), ethylene (Matheson Gas Products), and carbon monoxide (Matheson Gas Products) were used as received. Dicyclopentadiene (Fluka) was cracked immediately prior to use. Tetrabutylammonium hexafluorophosphate ($TBAPF_6$, puriss. from Fluka) was used as supporting electrolyte as received. Acetonitrile (CH_3CN, UVASOL, Merck) and tetrahydrofuran (THF, LiChrosolv, Merck) were treated according to a procedure described elsewhere.[31] For the electrochemical experiment, the solvents were distilled into the electrochemical cell, prior to use, using a trap-to-trap procedure.

4.2. UV−Visible Absorption and Fluorescence Emission Spectroscopy. The UV−visible absorption spectra were measured at room temperature in dinitrogen-saturated benzene solutions using a Cary 14 spectrophotometer with a resolution of 1 nm. The fluorescence properties at room temperature were measured on an ISS-GREG 200 multiphase fluorimeter with resolution of 2−4 nm in dinitrogen-saturated solutions at an absorbance of 0.1 at the excitation wavelength, i.e., ca. 360 nm. The emission spectra were not corrected for the instrumental response since they were all similar. The relative values of the fluorescence quantum yields were therefore obtained by comparison with the emission intensity of 9-methylanthracene, which has a quantum yield of 0.35 and a lifetime of 4.6 ns in cyclohexane.[32] The solvent Rayleigh scattering was used as an internal reference. All data have been normalized to the same absorbance at the excitation wavelength.

4.3. Electrochemical Instrumentation and Measurements. The one-compartment electrochemical cell was of airtight design with high-vacuum glass stopcocks fitted with either Teflon or Kalrez (DuPont) O-rings in order to prevent contamination by grease. The connections to the high-vacuum line and to the Schlenck containing the solvent were obtained by spherical joints also fitted with Kalrez O-rings. The pressure in the electrochemical cell, prior to performing the trap-to-trap distillation of the solvent, ranged typically from 1.0 to 2.0 $\times$ 10^{-5} mbar. The working electrode consisted of either a 0.6 mm diameter platinum wire (0.15 cm^2 approximately) sealed in glass or a platinum disk microelectrode (r = 125 μm) also sealed in glass. The counter electrode consisted of a platinum spiral, and the quasi-reference electrode was a silver spiral. The quasi-reference electrode drift was negligible for the time required by a single experiment. Both the counter and the reference electrode were separated from the working electrode by ~0.5 cm. Potentials were measured with the ferrocene standard and are always referred to saturated calomel electrode (SCE). $E_{1/2}$ values correspond to (E_{pc} + E_{pa})/2 from CV. For irreversible peaks, the peak potential, E_p, is given, measured at 0.5 V s^{-1}. Ferrocene was also used as an internal standard for checking the electrochemical reversibility of a redox couple. Voltammograms were recorded with an AMEL Model 552 potentiostat or a custom-made fast potentiostat controlled by either an AMEL Model 568 function generator or an ELCHEMA Model FG-206F. Data acquisition was performed by a Nicolet Model 3091 digital oscilloscope interfaced to a PC. Temperature control was accomplished within 0.1 °C with a Lauda Klein-Kryomat thermostat.

4.4. EPR Experiments. The X-band EPR spectra were obtained by a Varian E112 spectrometer controlling the temperature by an OXFORD EPR 900 cryostat. The EPR spectrometer was interfaced to an AT compatible computer by means of a data-acquisition system consisting of an acquisition board capable of acquiring up to 500 000 12-bit samples per second including 32-bit add to memory, thus giving on-line signal averaging,[33] and a software package specially designed for EPR experiments.[34] The EPR spectra were run by placing the sample (typically 30 μL) into quartz tubes (external diameter, 3 mm; internal diameter, 2 mm) fitted with a quartz-Pyrex joint and a Bibby Quickfit Rotaflo PTFE tap (Disa, Milan), according to already published procedures.[19] All the EPR experiments were run in a 1:1 (v/v) 1,1,1,3,3,3-hexafluoro-2-propanol/dichloromethane mixture. Both solvents were saturated with argon before use.

4.5. Synthesis of 9,10-Bis(cyclopentadienylmethyl)-anthracene (1). 9,10-Bis(bromomethyl)anthracene (0.99 g, 2.72 mmol) was added to a solution of cyclopentadienylsodium (0.59 g, 6.70 mmol) in tetrahydrofurane (18 mL) at −10 °C. The mixture was stirred at this temperature for 4 h and then filtered. The ochre-yellow solution obtained was dried under reduced pressure, at 0 °C. The residue was treated with benzene (15 mL), and the resulting suspension was filtered. The resulting solution was dried under reduced pressure, at 0 °C. The residue was dissolved in benzene (3 mL) and purified by column (internal diameter, 10 mm; length, 300 mm) chromatography on silica gel 60 (230−400 mesh) (Merck), using a 1:1 (v/v) chloroform/*n*-hexane mixture as eluant. The first ochre-yellow band that was eluted furnished 0.29 g of 9,10-bis(cyclopentadienylmethyl)anthracene as a yellow solid (0.87 mmol, 32% yield). Found: C, 93.35; H, 6.54. Anal. Calcd for $C_{26}H_{22}$: C, 93.41; H, 6.59. EI-MS, *m*/*z*: 334 $[M]^+$ (78%), 269 $[M - C_5H_5]^+$ (40%), 239 (15%), 191 (19%), 152 (13%), 82 (100%).

4.6. Synthesis of 9,10-Bis[(cyclopentadienylmethyl)-thallium(I)]anthracene (3). A mixture of 9,10-bis(cyclopentadienylmethyl)anthracene (2.29 g, 0.87 mmol), thallium(I) ethoxide (0.70 g, 2.82 mmol), and absolute ethanol (60 mL) was stirred for 4 h, at room temperature. An ochre-yellow solid precipitated, which was separated by decanting off the supernatant solution, washed with absolute ethanol (2 $\times$ 15 mL), then with dry diethyl ether (2 $\times$ 15 mL) and with pentane (2 $\times$ 15 mL), and finally dried under vacuum; 0.37 g of the title compound (0.5 mmol, 57% yield), as an ochre-yellow microcrystalline solid, was obtained. Found: C, 58.08; H, 3.61. Anal. Calcd for $C_{26}H_{20}Tl_2$: C, 58.19; H, 3.73. Owing to the toxicity of the thallium derivatives, the compound **3** must be handled with care.

4.7. Synthesis of 9,10-Bis[(η^5-cyclopentadienylmethyl)-bis(η^2-ethylene)rodium(I)]anthracene (4). A mixture of 9,10-bis[(cyclopentadienylmethyl)thallium(I)]anthracene (0.17

(25) King, R. B.; Stone, F. G. A. *Inorg. Synth.* **1963**, *7*, 99.
(26) McCleverty, J. A.; Wikinson, G. *Inorg. Synth.* **1966**, *8*, 211.
(27) Cramer, R. *Inorg. Chem.* **1962**, *1*, 722.
(28) Abel, E. W.; Bennett, M. A.; Wilkinson, G. *J. Chem. Soc. (A)* **1959**, 3178.
(29) King, R. B. *Inorg. Chem.* **1963**, *2*, 528.
(30) Evans, J.; Johnson, B. F. G.; Lewis, J. *J. Chem. Soc., Dalton Trans.* **1977**, 510.
(31) Carano, M.; Ceroni, P.; Mottier, L.; Paolucci, F.; Roffia, S. *J. Electrochem. Soc.* **1999**, *146*, 3357.
(32) Berlman, I. *Handbook of fluorescence spectra of aromatic molecules*; Academic Press: New York, 1965.
(33) Ambrosetti, R.; Ricci, D. *Rev. Sci. Instrum.* **1991**, *62*, 2281.
(34) Pinzino, C.; Forte, C. *EPR-ENDOR, ICQEM-CNR Pisa*; 1994.

g, 0.23 mmol), di-μ-chlorotetrakis(η^2-ethylene)dirodium(I) (0.10 g, 0.26 mmol), and benzene (13 mL) was stirred for 1.5 h at room temperature and then filtered. The resulting solution was dried under reduced pressure. The residue was dissolved in 2 mL of a benzene/*n*-hexane (1:1, v/v) mixture and purified by column (internal diameter, 10 mm; length, 30 mm) chromatography on alumina (aluminum oxide 90, 70−230 mesh, MERCK), using a 1:1 (v/v) benzene/*n*-hexane mixture as eluant, under dinitrogen atmosphere. From the first orange-yellow band that eluted, 0.02 g of the title compound (0.03 mmol, 13%, yield) was obtained as an orange-yellow microcrystalline powder. Found: C, 62.57; H, 5.50. Anal. Calcd for $C_{43}H_{36}Rh_2$: C, 62.80; H, 5.54.

4.8. Synthesis of 9,10-Bis[(η^5-cyclopentadienylmethyl)-dicarbonylrhodium(I)]anthracene (5). A mixture of 9,10-bis[(cyclopentadienylmethyl)thallium(I)]anthracene (0.27 g, 0.36 mmol), di-μ-chlorotetrakis(carbonyl)dirodium(I) (0.14 g, 0.36 mmol), and benzene (22 mL) was stirred for 2 h, at room temperature and then filtered. The resulting solution was dried under reduced pressure. The residue was dissolved in 2 mL of benzene and purified by column (internal diameter, 10 mm; length, 30 mm) chromatography on alumina (aluminum oxide 90, 70−230 mesh, MERCK), using a 7:3 (v/v) benzene/*n*-hexane mixture as eluant, under dinitrogen atmosphere. From the first orange band that eluted, 0.05 g of the title compound (0.08 mmol, 22%, yield) was obtained as an orange-yellow microcrystalline powder. Found: C, 55.36; H, 3.01. Anal. Calcd for $C_{30}H_{20}O_4Rh_2$: C, 55.42; H, 3.08. IR CO stretching (Nujol): 2042 (w), 1979 (w) cm^{-1}.

4.9. Synthesis of 9,10-Bis[(η^5-cyclopentadienylmethyl)-(η^4-norbornadiene)rhodium(I)]anthracene (6). A mixture of 9,10-bis[(cyclopentadienylmethyl)tallium(I)]anthracene (0.26 g, 0.35 mmol), di-μ-chlorobis(η^4-norbornadiene)dirodium(I) (0.15 g, 0.32 mmol), and benzene (50 mL) was stirred for 3 h, at room temperature, and then filtered. An orange-red solution was obtained, which was dried under reduced pressure. The residue was dissolved in 3 mL of benzene and purified by column (internal diameter, 10 mm; length, 30 mm) chromatography on alumina (aluminum oxide 90, 70−230 mesh, MERCK), using a 3:7 (v/v) benzene/*n*-hexane mixture as eluant, under dinitrogen atmosphere. From the second yellow band that eluted, 0.14 g of the title compound (0.19 mmol, 55% yield) was obtained as a yellow solid. Found: C, 66.43; H, 4.90. Anal. Calcd for $C_{40}H_{36}Rh_2$: C, 66.52; H, 4.99.

Acknowledgment. Financial support from the MURST (Rome, Italy) and from the University of Bologna (Funds for Selected Research Topics) is gratefully acknowledged.

OM010206O